Functional role of NSP-like 1 protein in membrane translocation of glucose transporter 4

Takaaki Ikemoto,[1] Takamitsu Hosoya,[2] Kumi Takata,[1] Hiroshi Aoyama,[3] Toshiyuki Hiramatsu,[2] Hirotaka Onoe,[1] Masaaki Suzuki,[4] and Makoto Endo[5]

Supplemental RESEARCH DESIGN AND METHODS

Isolated membranes from skeletal muscles

Muscles were homogenized in a solution containing Na pyrophosphate (20 mmol/l) and EDTA (1 mmol/l) with 7.5% sucrose (buffer A). The homogenate was centrifuged at 1,300 × *g* for 10 min, and the supernatant was further centrifuged at 100,000 × *g* for 1 h. The resulting pellet (crude membrane, CM) was resuspended in buffer A containing 1.0 mol/l NaCl and applied on discontinuous sucrose gradients (25 and 35%, w/w) and centrifuged at 100,000 × *g* for 90 min. Membranes at the 7.5% intermediate (F1), 7.5/25% (F2), and 25/35% (F3) interfaces were recovered and diluted with 20 mmol/l PIPES/Tris (pH 7.0) and centrifuged at 100,000 × *g* for 1 h. The pellet from the centrifuging the initial homogenate was resuspended in buffer B (0.5 mol/l LiBr, 50 mmol/l Tris, pH 8.5) and stirred for 3-4 h. The LiBr-treated membranes were centrifuged first at 1,300 × *g* for 10 min, then at 52,000 × *g* for 30 min and again at 100,000 × *g* for 1 h (Li-M). All pellets were resuspended in the final buffer (0.3 mol/l sucrose, 0.1 mol/l KCl, 20 mmol/l PIPES/Tris, pH 7.0).

When fractional change of GLUT4 induced by insulin was observed, insulin (2U) was injected 30 min before isolation of muscles. When the change of GLUT4 induced by contraction was observed, electrical stimulation (20 V, 0.5 ms duration, 25 Hz for 2 s, 3 s^{-1}) was applied for 15 min through electrodes directly inserted into the hindlimbs, and then the muscles were quickly isolated. GLUT4, DHPα2, Na-K ATPase, actin, and mouse NSPl1 proteins in CM, F1, F2, F3, and Li-M fractions were quantified with their corresponding antibodies (Chemicon and Affinity BioReagents) and AP-conjugated secondary antibodies (Promega) on PVDF membranes after SDS-PAGE.

Microsome fraction from tissues other than skeletal muscles

Microsome fractions from cardiac muscle, small intestine, and whole brain were obtained in accordance with a previous report (suppl. ref. 1). Expression levels of GLUT4, actin, and mouse NSPl1 proteins in cardiac muscle, small intestine, and whole brain were compared using their corresponding antibodies (Chemicon and Sigma) and AP-conjugated secondary antibodies (Promega) on PVDF membranes after SDS-PAGE.

Supplemental Reference

1. Stevens SM Jr, Duncan RS, Koulen P, Prokai L. Proteomic analysis of mouse brain microsomes: identification and bioinformatic characterization of endoplasmic reticulum proteins in the mammalian central nervous system. *J Proteome Res*. 2008; 7, 1046–1054

FIG. S1. Structures of dantrolene derivatives and their effect on Ca^{2+} release

A: Structure of dantrolene sodium (Dan). *B*: *N*-(3-Azido-5-iodo)benzylated Dan derivative, which is referred to as GIF-0082, was designed as a photoaffinity probe with an azido group as a photoreactive unit and iodine as a latent radioisotope group (iodine-125). *C*: GIF-0136. *D*: GIF-0166. *E*: GIF-0192. *F*: GIF-0430. *G*: GIF-0430 with a bifunctional unit consisting of a photoreactive function and an aliphatic azide group was coupled with fluorescent triarylphosphine derivative GIF-0373 (500 µmol/l) by Staudinger-Bertozzi ligation. Syntheses of these compounds were previously reported in detail (20-23). *H*: Photo-affinity labeling of [^{125}I]GIF-0136 in the TC fraction from mouse skeletal muscles. Samples were mixed with 600 nmol/l [^{125}I]GIF-0136 and photo-irradiated with UV light in the absence (lane 1) or presence of GIF-0082 (lanes 2 and 3, 7 µmol/l and 15 µmol/l GIF-0082, respectively; lane 4, 7 µmol/l Dan). Unlike [^{125}I]GIF-0082 (Fig. 1*A*), GIF-0136 did not recognize the protein exhibiting an apparent molecular weight of 23 kDa. *I-K*: Functional differences of Dan derivatives (GIFs) in normal skeletal muscles. The sizes of twitch contraction after treatment of GIFs were compared with that before treatment in intact muscle (100%, *I*). In skinned fibers, the rates of Ca^{2+} release measured with GIFs were normalized by the control value (without GIFs, *J* and *K*). GIF-0136 showed little inhibition on twitch tension (*I*, n = 3-8) or on the Ca^{2+}-induced Ca^{2+} release (CICR, at 1 µmol/l Ca^{2+}, Mg^{2+}-free) mechanism (*J*, n = 3-8). Thus it could not affect the two types of Ca^{2+} release mechanisms in skeletal muscle (27, 31). Since the reduction of pharmacological effect of Dan derivatives on Ca^{2+} release might result from the lowered binding activity with the 23 kDa protein (sk-NSPl1), we hoped to elucidate the unknown mechanism in excitation-contraction coupling, on the basis of the sk-NSPl1 function. GIF-0166 was a unique Dan derivative that increased the rate of Ca^{2+} release about 2-fold (50 µmol/l) in skinned skeletal muscle at 1 µmol/l Ca^{2+} (*J*, *K*). Thus CICR was potentiated by the derivative, although physiological Ca^{2+} release was not inhibited (*I*). GIF-0192, another type of Dan derivative, showed no effect on either type of Ca^{2+} release (*I* and *J*); on the other hand, the GIF-0166-induced increase of Ca^{2+} release rates was reduced by the presence of GIF-0192 (100 µmol/l, *K*). Thus, GIF-0192 antagonized the effect of GIF-0166. We thought that these Dan derivatives may affect CICR in a different mechanism with Dan; however, both bind with sk-NSPl1, which might have biphasic, inhibitory, and enhancing effects on Ca^{2+} release, similar to calmodulin (26).

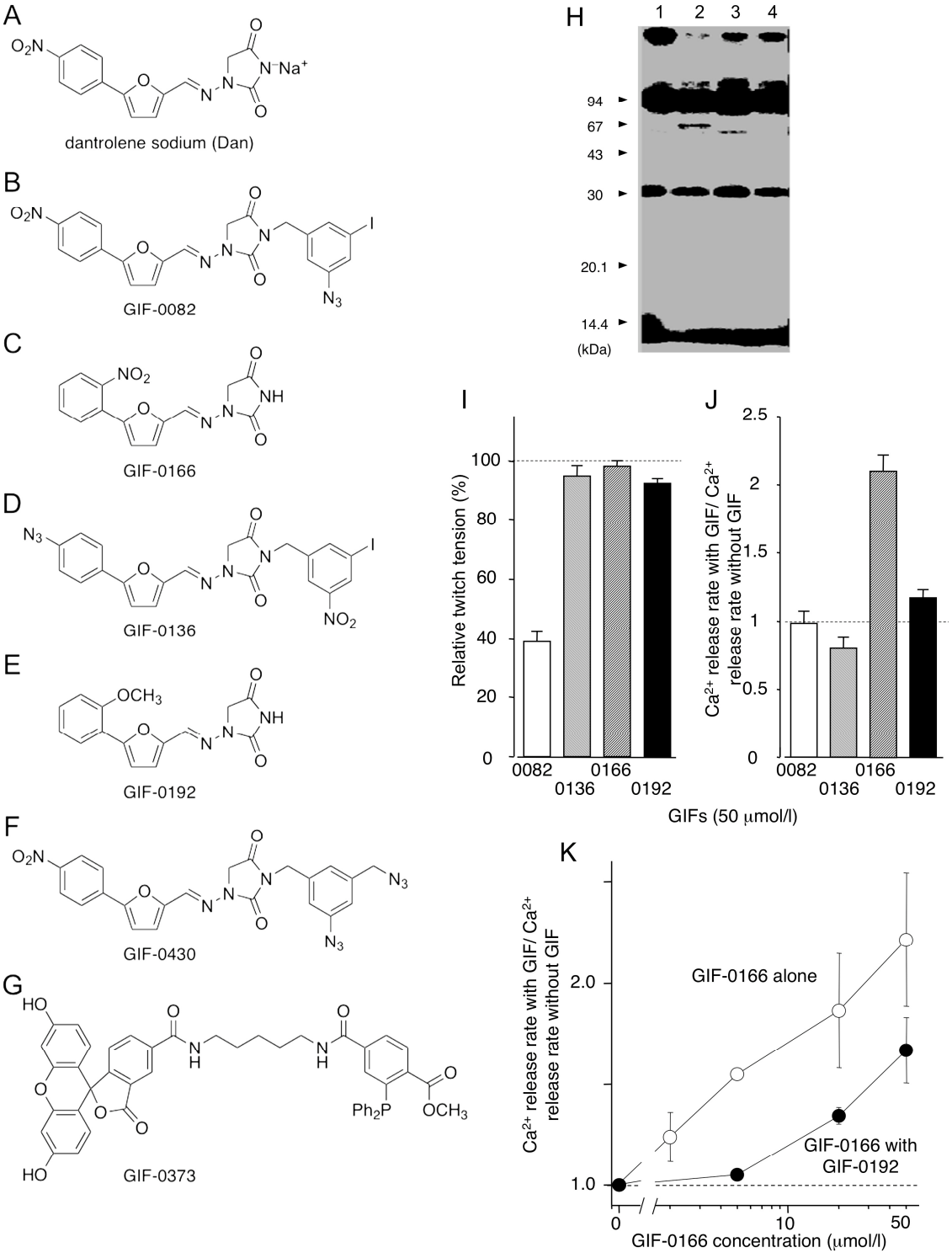
A
dantrolene sodium (Dan)
B
GIF-0082
C
GIF-0166
D
GIF-0136
E
GIF-0192
F
GIF-0430
G
GIF-0373
H
1 2 3 4
94
67
43
30
20.1
14.4
(kDa)
I
Relative twitch tension (%)
0082
0166
0136
0192
J
Ca2+ release rate with GIF/ Ca2+ release rate without GIF
GIFs (50 μmol/l)
K
Ca2+ release rate with GIF/ Ca2+ release rate without GIF
GIF-0166 alone
GIF-0166 with GIF-0192
GIF-0166 concentration (μmol/l)

FIG. S2. Ca^{2+} release in sk-NSPl1-deficient skeletal muscles

A, B: Tension-frequency relationship of diaphragm (*A*, *n* = 8) and extensor digitorum longus (EDL) (*B*, *n* = 6-7) muscle from wild-type (open circles, open squares) or sk-NSPl1-deficient (filled circles, filled squares) mice at 37 °C. The relative force was calculated by counting the force recorded at a stimulus frequency of 125 Hz as 100%. The frequency-tension relationship was unchanged in deficient skeletal muscles. *C*: Ca^{2+} release measured in saponin-treated skinned EDL muscle from sk-NSPl1-deficient mice at room temperature (22-24 °C). The rates of Ca^{2+} release were measured at 0.1 or 1.0 µmol/l Ca^{2+} with or without Dan (20 µmol/l) under Mg^{2+}-free conditions (*n* = 3). The Ca^{2+} release rates increased at high concentrations of Ca^{2+}. Therefore the CICR mechanism was also preserved in sk-NSPl1-deficient cells, indicating that the Ca^{2+} release mechanisms is functionally intact in the mutant.

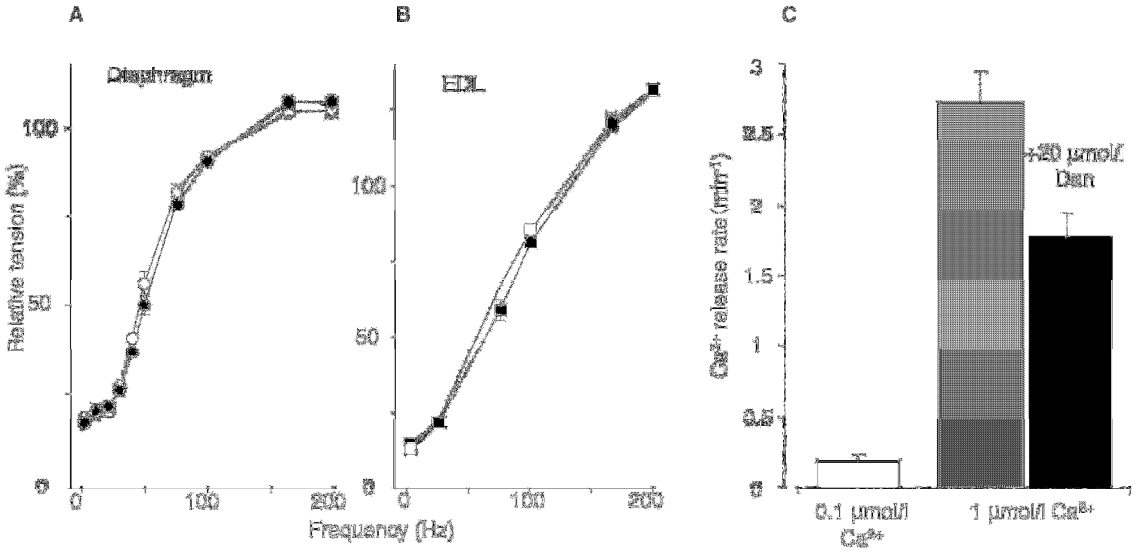

FIG. S3. Effect of glucose during [^{18}F]FDG uptake in muscles

After recording contractions evoked by electrical stimulation (125 Hz for 320 ms, 3 s^{-1}) in the normal glucose solution, skeletal muscles were washed with glucose-free solution, then incubated in solution containing [^{18}F]FDG for 5 min in the presence or absence of 5.6 mmol/l glucose (n = 3-5). Uptake of [^{18}F]FDG without stimulation did not change in the presence or absence of glucose, while uptake with stimulation was markedly reduced by the presence of glucose (5.6 mmol/l). Glucose might be a competitor of [^{18}F]FDG entry into the cell via GLUT4. Therefore, our protocol incorporated stimulation to induce GLUT4 translocation in the presence of glucose, while measuring the uptake of [^{18}F]FDG into the cell in the absence of glucose (Fig. 3).

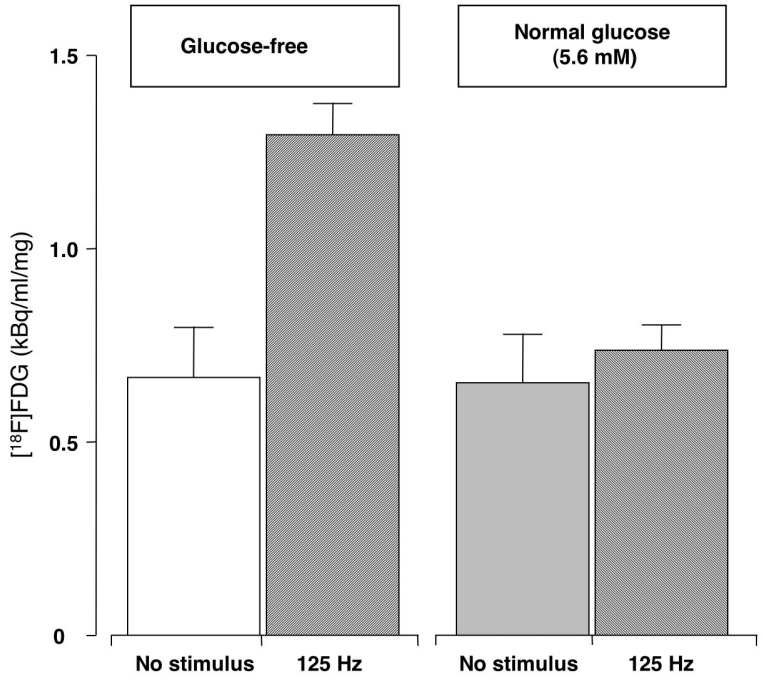

FIG. S4. Localization of NSPl1 protein in the mouse skeletal muscle

Localization of NSPl1 protein in wild-type (*A*, *B*, *E*) or sk-NSPl1-deficient (*C*, *D*, *F*) muscles. Distributions of NSPl1 protein were compared with those of actin which was labeled with fluorescent phalloidin. Confocal imaging was obtained for the cell surface (*A* and *E*; *C* and *F*) or in the middle section of the cell (*B* and *D*) as indicated by the filled white arrowhead in each cross-section. Open arrowheads represent the dimension of the obtained cross-section. NSPl1/actin represents double staining and imaging with two channels; NSPl1 and actin separately represent imaging from a single channel (fluorescence from Alexa Fluor 568 or 488) in the same preparation. Yellow arrow, longitudinal strand derived NSPl1 protein (*B*). Bar = 5 μm. Characteristic locations of NSPl1 proteins were superimposed in *E* and *F*. Each inset in *E* and *F* indicates the signal from NSPl1 protein labeled with Alex Fluor 568 alone. Bar = 1 μm.

In muscles from wild-type mice, NSPl1 was detected abundantly near the sarcolemma not only over the Z-lines as reported previously (38), but also in much more widely spread regions (Fig. S4*A*). There were longitudinal strands as well, and transverse elements spanned

over the whole region where actin is present (Fig. S4*A* and S4*E*). In the deep sections of cells, NSPl1 was also broadly distributed with actin, and in some parts longitudinal strands were also present (Fig. S4*B*, yellow arrow). In sk-NSPl1-deficient muscle, the transverse elements over the Z-lines derived from NSPl1 disappeared in deep cell sections (Fig. S4*D*) as expected, and there were also no longitudinal strands (Fig. S4*C* and S4*F*). On the other hand, near the sarcolemma, even in NSPl1-deficient muscle, transverse elements were detectable (Fig. S4*C* and S4*F*) in the region, where actin does not exist. The protein remaining near the sarcolemma may be a brain type of NSPl1 (18), since we deleted the skeletal type only, while our specific antibody was raised against the C-terminus of NSPl1, which is common to both types of NSPl1 (18). Since the fluorescence intensities from our antibody were greatly diminished in the mutant mouse (Fig. S4*A* vs. S4*C*), both types of NSPl1 might be expressed near the sarcolemmal membrane of skeletal muscles. However, we could not detect the brain type in microsomes and Li-extracted fractions from muscles (Fig 1*E*). This indicated that another type of NSPl1 is present at a low level in skeletal muscles. In addition, fluorescence from NSPl1 appeared on the nuclear membrane in both wild-type (data not shown) and mutant cells (Fig. S4*C* and S4*D*).

Thus these images suggested that native sk-NSPl1 has a complex distribution in skeletal muscle cells, not confined to the Z-line (47), and that other type(s) of NSPl1 are most likely expressed in skeletal muscle cells.